Since January 2020 Elsevier has created a COVID-19 resource centre with free information in English and Mandarin on the novel coronavirus COVID-19. The COVID-19 resource centre is hosted on Elsevier Connect, the company's public news and information website.

Colloids and Surfaces A 608 (2021) 125564

Contents lists available at ScienceDirect

Colloids and Surfaces A

journal homepage: www.elsevier.com/locate/colsurfa

Morphology and protein adsorption of aluminum phosphate and aluminum hydroxide and their potential catalytic function in the synthesis of polymeric emulsifiers

Yu-Jhen Cheng[a,1], Chiung-Yi Huang[a,1], Hui-Min Ho[a], Ming-Hsi Huang[a,b,c,d,*]

[a] National Institute of Infectious Diseases and Vaccinology, National Health Research Institutes, 35053 Miaoli, Taiwan
[b] Graduate Institute of Biomedical Sciences, China Medical University, 40402 Taichung, Taiwan
[c] Graduate Institute of Medicine, Kaohsiung Medical University, 80708 Kaohsiung, Taiwan
[d] Biotechnology Center, National Chung Hsing University, 40227 Taichung, Taiwan

GRAPHICAL ABSTRACT

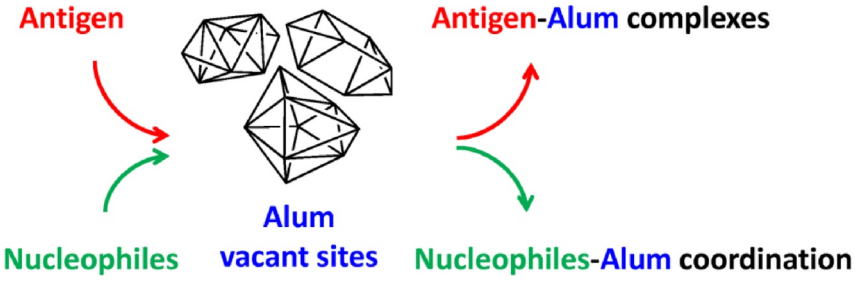

ARTICLE INFO

Keywords:
Adsorption
Aluminum-containing adjuvants
Melt-solid polycondensation
Oil-in-water emulsion
Polymeric emulsifiers

ABSTRACT

Aluminum-containing salts are commonly used as antacids and vaccine adjuvants; however, key features of functional activities remain unclear. Here, we characterized vaccine formulations based on aluminum phosphate and aluminum hydroxide and investigated the respective modes of action linking physicochemical properties and catalytic ability. TEM microscopy indicated that aluminum phosphate gel solutions are amorphous, whereas aluminum hydroxide gel solutions have a crystalline structure consistent with boehmite. At very low BSA concentrations, 100 % adsorption of the protein on aluminum hydroxide could be achieved. As the protein concentration increased, the amount of adsorbed BSA decreased as fewer vacant sites were available on the surface of the adjuvants. Notably, less than 20 % adsorption was observed in aluminum phosphate. The protein adsorption profiles should confront the requirements for vaccine immunoavailability. In terms of catalytic ability, the prepared aluminum salts were tested for their ability to drive the amphiphilic engineering of oligo (lactic acid) (OLA) onto methoxy poly(ethylene glycol). It was concluded that aluminum hydroxide, rather than aluminum phosphate, is suitable to be a vaccine adjuvant according to the morphology and antigen adsorption efficiency results; on the other hand, aluminum phosphate may be a more efficient catalyst for the synthesis of polymeric emulsifiers than aluminum hydroxide. The results provide critical mechanistic insight into aluminum-containing salts in vaccine formulations.

* Corresponding author at: National Institute of Infectious Diseases and Vaccinology, National Health Research Institutes (NHRI), Taiwan.
E-mail address: huangminghsi@nhri.org.tw (M.-H. Huang).
[1] These authors contributed equally to this work.

https://doi.org/10.1016/j.colsurfa.2020.125564
Received 16 June 2020; Received in revised form 30 July 2020; Accepted 3 September 2020
Available online 10 September 2020

1. Introduction

The influenza A (H1N1) virus of swine origin described in 2009 and severe acute respiratory syndrome coronavirus 2 (SARS-CoV-2) that appeared in 2019 are causing a global pandemic in this century [1,2]. Vaccination is considered a promising strategy for inducing protective immunity against pathogen infections [2]. However, a highly purified antigen applied to certain populations sometimes induces miniscule immune responses owing to immune tolerance. Therefore, the aid of a safe vaccine adjuvant with high efficacy is necessary for antigen recognition by the immune system and the generation of broad-spectrum and long-lasting immune responses [3]. Aluminum-containing salts and squalene-based emulsified droplets are currently licensed adjuvants for human vaccines [3–6]. Following vaccination, both of them enhance the antigen-specific immune responses by triggering the inflammation at the injection site and promoting the cell-mediated trafficking of antigen to the draining lymph nodes [3,7,8]. These antigen-loaded antigen-presenting cells (APCs) then facilitated T cell and B cell responses [3,8]. Another aspect of the aluminum adjuvants is to create the delivery vehicles (as depot/carriers) in order to either adsorb the antigens along with the designed bioactive molecules or protect them from degradation [9,10]. For the feasibility study on adjuvant optimization for the development of next-generation vaccines, it is important to obtain more comprehensive information on protein adsorption properties associated with the structure of different forms of gel suspensions. It is also of interest to obtain integrative information on their potential function in combination with a squalene emulsion for vaccine development.

Previously, we reported on the pioneering work of engineering amphiphilic bioresorbable polymers as emulsifying agents to diminish the surface energy at oil/water interfaces, resulting in the formation of emulsified vesicles [11–13]. The emulsified vesicles thus obtained were demonstrated to be potential sustained-release depots for inactivated viruses [11], peptides [12] and proteins [13], thereby introducing microencapsulation technology for the development of emulsion adjuvants in prophylactic and therapeutic vaccines against infectious diseases and cancers [11,12]. However, a high rate of conversion from ester monomotifs to polymers with a high yield of polymer recovery requires the presence of cytotoxic catalyst-containing heavy metals [12,13], and thus, favorable conditions for polymerization should still be optimized.

The present study aims to deepen our understanding of aluminum-containing salts by providing comprehensive information on depot potency of these salts as vehicles to increase adsorption capacity and integrative information on the functional efficacy of these materials as catalysts to facilitate emulsifier synthesis. Two commercially available aluminum-containing salts, labeled aluminum hydroxide and aluminum phosphate, were evaluated in this study. We report on the relationship between the morphology and protein adsorption profiles of aluminum hydroxide and aluminum phosphate using bovine serum albumin (BSA) as a model protein. In parallel, we also evaluate the potential catalytic function of these salts in the synthesis of the polymeric emulsifier PEG–PLA by polycondensation of lactic acid oligomers onto methoxy PEG using aluminum hydroxide or aluminum phosphate as a catalyst. The resulting products were first subjected to molecular weight characterization using size-exclusion chromatography (SEC); in addition, the amphiphilic properties were tested in terms of the ability to stabilize the interfaces between the aqueous solution and water-immiscible squalene oil. The results were compared with those obtained without a catalyst or with a conventional $SnOct_2$ catalyst.

2. Materials and methods

2.1. Physicochemical characterization

Aluminum hydroxide ($Al(OH)_3$, Alhydrogel®) and aluminum phosphate ($AlPO_4$, Adju-Phos®) wet gel suspensions were purchased from InvivoGen (San Diego, USA). The microscopic characteristics were monitored using transmission electron microscopy (H-7650, Hitachi, Japan). X-ray diffraction patterns were obtained with a Shimadzu apparatus (Miniflex II, Rigaku, Tokyo, Japan) using a Cu-Kα source, and the diffraction patterns were recorded from 10 to 80° with a resolution of 1°. To prepare aluminum-based adjuvants with adsorbed antigens, a 2-mL suspension containing 1,000 μg of aluminum content of $Al(OH)_3$ or $AlPO_4$ was incubated with 100 − 2,000 μg BSA protein (Cyrusbioscience, New Taipei City, Taiwan) in PBS and left on an orbital shaking incubator at 180 rpm for 3 h and then precipitated by centrifugation at 1,000 rpm for 5 min. Samples (200 μL) were aspirated from the clear supernatant layer above the precipitates, and the BSA protein content was measured by a BCA™ protein assay kit (Pierce, Rockford, IL, USA).

2.2. Polymer synthesis

Lactic acid solution (85–90 %) was sourced from Sigma-Aldrich (St. Louis, MO, USA). Oligo(lactic acid) (OLA) was prepared by simple distillation of lactic acid solution for 3 h at 140 °C by means of a central suction system operated on a rotary evaporator (Rotavapor® R-210, Buchi Labortechnik AG, Switzerland), as previously described [14]. Poly(ethylene glycol) monomethyl ether with an average molecular weight of 2,000 ($MePEG_{2000}$) and tin(II) 2-ethylhexanoate ($SnOct_2$) were supplied by Sigma (St. Louis, MO, USA). The $Al(OH)_3$ and $AlPO_4$ gel suspensions were lyophilized before being subjected to polymerization.

PEG–PLA was synthesized by melt polycondensation of OLA with $MePEG_{2000}$ [14]. Equal amounts of OLA (9 g) and $MePEG_{2000}$ (9 g) were charged into a round-bottom flask and mixed with a predetermined amount (ca. 0.5 %) of $SnOct_2$ or aluminum content of $Al(OH)_3$ or $AlPO_4$. Polymerization was carried out at 170 °C for 6 h. After the reaction was cooled and the products were solidified, the products were recovered and stored in a desiccator under vacuum.

The molecular weight (MW) characteristics of the polymers were determined by SEC. The chromatograph instruments were equipped with size exclusion columns (Agilent Technologies, Inc., UK), connected to an HPLC pump with the mobile phase of THF at a flow rate of 0.8 mL/min, and monitored continuously using a refractive index (RI) detector (LabAlliance™ RI-101, Scientific System Inc., USA). The peak MW (M_p), number-average MW (M_n) and dispersity index (I_p) were calibrated relative to those of polystyrene standards (Varian, Inc., Amherst, MA, USA). The emulsifying property was evaluated by homogenizing liquid-liquid binary phases comprising 0.6 mL of phosphate-buffered saline (HyClone Laboratories, South Logan, Utah, USA) and 1.6 mL of squalene oil (Sigma-Aldrich, St. Louis, MO, USA) in the presence of 150 mg of the recovered polymers. Emulsification was conducted with a homogenizer (Polytron® PT 2500, Kinematica AG, Switzerland) operated at 6,000 rpm for 5 min. The microscopic characteristics were assessed using an Olympus DP70 microscope, and the particle size distribution was determined by a particle size analyzer (Malvern 90plus with zetaPALS, Brookhaven Instruments, NY, USA).

3. Results and discussion

3.1. Morphology and protein adsorption

Besides inflammation, it has been shown that aluminum crystals also induce an abortive phagocytic response that leads to antigen uptake [4]; furthermore, antigen absorption on the surface of aluminum-based adjuvants has the prospect to play an important role in manipulating antigen availability for the antigen-presenting cells at the injection site [7]. Thus, we studied the morphology and protein adsorption isotherms of $Al(OH)_3$ and $AlPO_4$.

The morphology of $Al(OH)_3$ and $AlPO_4$ was characterized by TEM

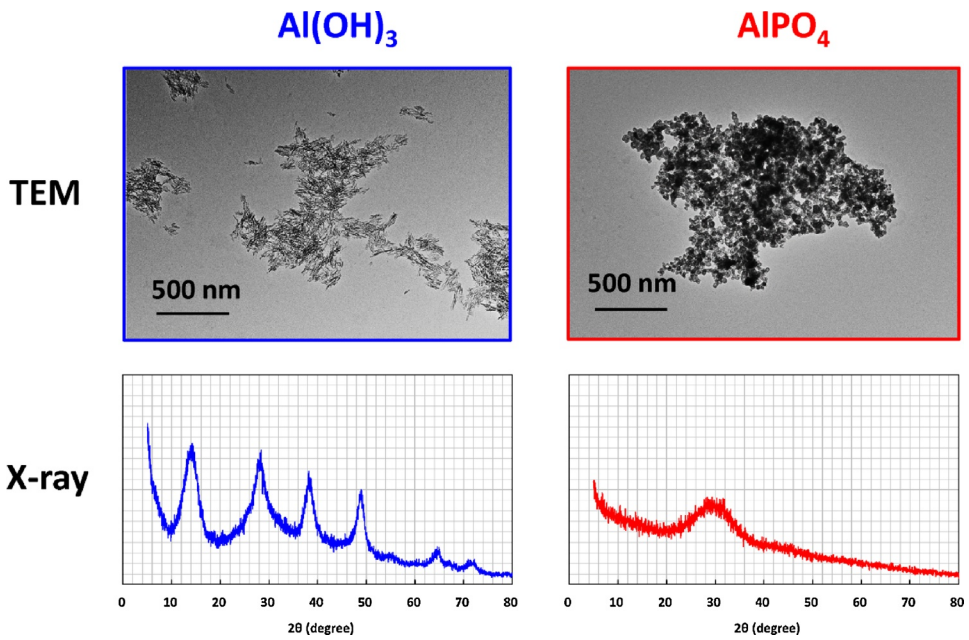

Fig. 1. TEM morphology and X-ray diffraction patterns of $Al(OH)_3$ and $AlPO_4$.

and X-ray diffraction, as shown in Fig. 1. A fibrous morphology could be seen in adjuvant $Al(OH)_3$ but not in $AlPO_4$. $Al(OH)_3$ gave rise to X-ray diffraction bands at $2\theta = 14^\circ$, 28°, 38°, 49°, 55°, 65°, and 72°, showing good agreement with the crystalline structure of boehmite [15,16]. In contrast, no characteristic diffraction peaks of boehmite were detected in the spectrum of $AlPO_4$. Our findings indicate that $AlPO_4$ gel solutions are amorphous, whereas $Al(OH)_3$ gel solutions have a crystalline structure consistent with boehmite.

The percentage of BSA protein adsorption onto the aluminum-based adjuvants was calculated according to the following equation:

$$\text{Protein adsorption (\%)} = 100(W_i - W_s)/W_i$$

where W_s and W_i represent the supernatant protein content after in situ adsorption and the initial protein content, respectively. Fig. 2A shows the BSA protein adsorption profiles of the $Al(OH)_3$ gel suspensions. At low BSA concentrations, 100 % adsorption of the protein could be achieved, and the adsorption percentage was not sensitive to the pH or temperature. As the protein concentration increased (antigen/adjuvant ratio > 0.6), BSA adsorption was inversely proportional to the antigen/adjuvant ratio, probably due to fewer vacant sites being available on the surface of the adjuvants. When the antigen/adjuvant ratio was between 0.6 and 2.0, the adsorption of BSA onto the $Al(OH)_3$ gel was not sensitive to the temperature, whereas the gel was capable of adsorbing more BSA at a pH of 6.0 than at a pH of 7.4. It should be noted that the pH affects adsorption by adjusting the charge on the antigens and adjuvants, whereas the temperature may have an effect on the rate of precipitation and interaction, as described in the literature [5,17]. The adsorption profiles of BSA are strongly influenced by the presence of $AlPO_4$ or $Al(OH)_3$. The data in Fig. 2B revealed that BSA protein molecules do not adsorb well onto $AlPO_4$, where less than 20 % adsorption was observed whatever the testing conditions. The protein adsorption profiles should confront the requirements for vaccine immunoavailability.

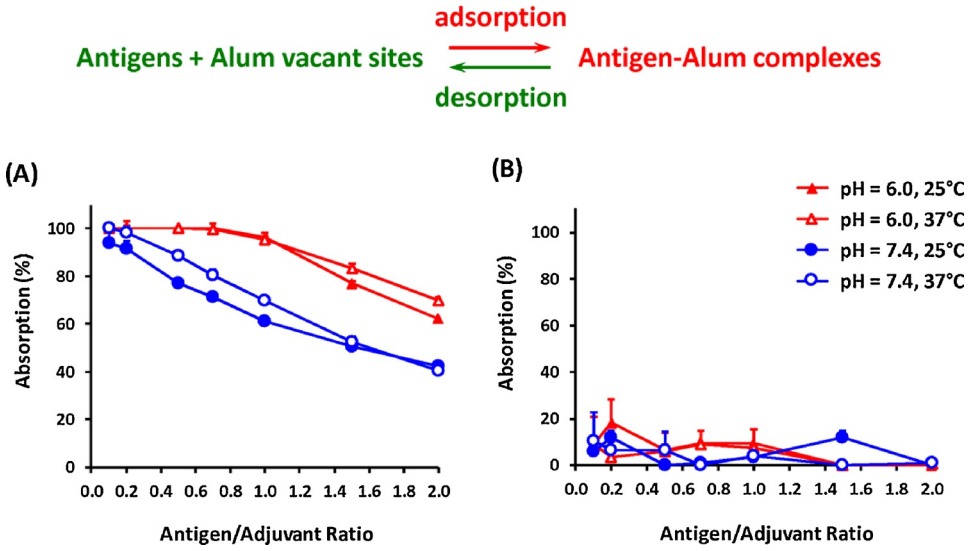

Fig. 2. Relationship between the antigen/adjuvant ratio and protein adsorption isotherm of bovine serum albumin with **(A)** $Al(OH)_3$ and **(B)** $AlPO_4$.

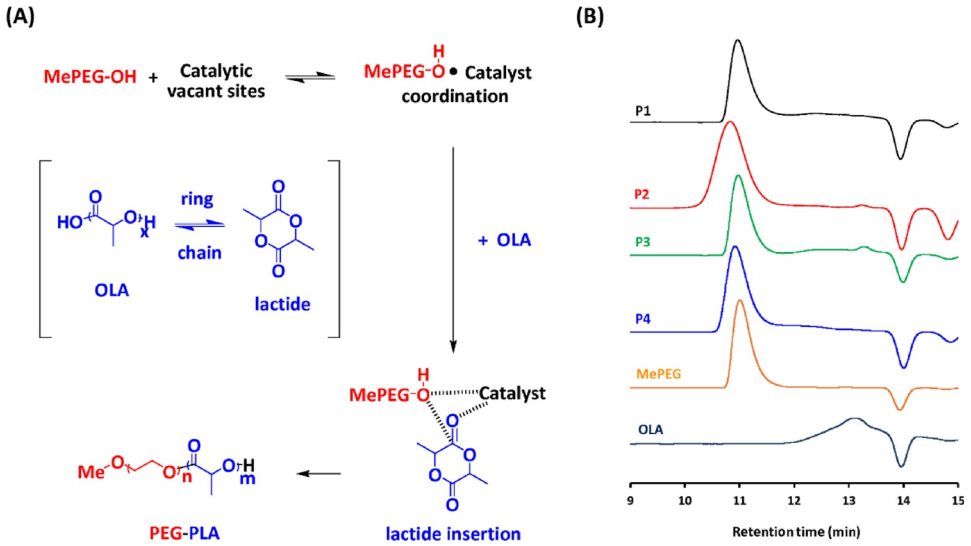

Fig. 3. (A) Schematic representation and **(B)** molecular weight distribution of PEG–PLA copolymers prepared by different catalysts. P1: no catalyst, P2: catalyzed by $SnOct_2$, P3: catalyzed by $Al(OH)_3$, and P4: catalyzed by $AlPO_4$.

Table 1
Physicochemical characteristics of PEG–PLA emulsifiers and PEG–PLA-based emulsions.

Sample	Polymer	Catalyst	M_p (Da)	M_n (Da)	I_p	Particle Size
P1	PEG–PLA	No catalyst	3,150	1,840	1.42	–
P2	PEG–PLA	$SnOct_2$	3,760	3,300	1.15	~1 μm
P3	PEG–PLA	$Al(OH)_3$	3,120	1,740	1.52	–
P4	PEG–PLA	$AlPO_4$	3,350	2,200	1.32	~1–20 μm, < 1 μm
–	$MePEG_{2000}$	–	2,980	2,500	1.10	–
–	OLA	–	185	180	1.33	–

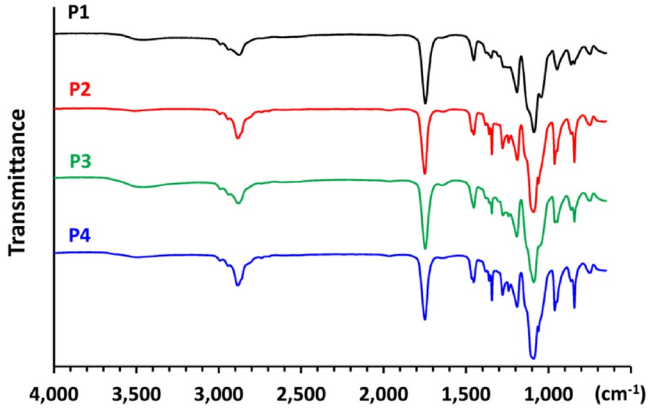

Fig. 4. IR spectra of PEG–PLA copolymers prepared by different catalysts, where the sample was placed on a ZnSe plate. P1: no catalyst, P2: catalyzed by $SnOct_2$, P3: catalyzed by $Al(OH)_3$, and P4: catalyzed by $AlPO_4$.

3.2. Catalytic function

For the synthesis of PEG–PLA, equivalent amounts of OLA and MePEG were introduced into the reactor as the starting materials in the presence of the candidate catalysts $SnOct_2$, $Al(OH)_3$ and $AlPO_4$. Since chain extension of OLA onto methoxy PEG occurred at one hydroxyl end only, the rendered product had a proposed chain structure of di-block copolymer PEG–PLA (Fig. 3A). The physicochemical characteristics of the designed polymeric emulsifiers and the obtained emulsions are summarized in Table 1.

The SEC results (Fig. 3B) showed that noncatalyzed (sample P1) or

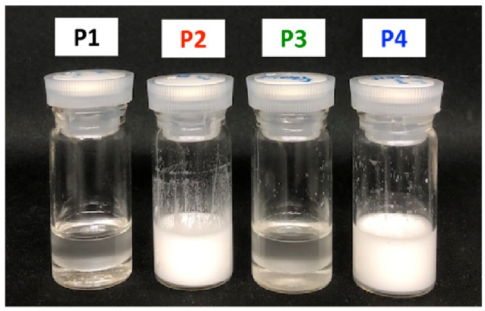

Fig. 5. Visual characterization of the designed formulations. Aqueous: water; core oil: squalene; emulsifiers: PEG–PLA without a catalyst (sample P1) and PEG–PLA made by $SnOct_2$ (sample P2), $Al(OH)_3$ (sample P3), or $AlPO_4$ (sample P4) catalysis.

$Al(OH)_3$-catalyzed formation of PEG–PLA (sample P3) resulted in a broad MW distribution, probably due to the presence of free OLA species. The I_p values were 1.42 and 1.52 for samples P1 and P3, respectively. On the other hand, $SnOct_2$-catalyzed formation of PEG–PLA (sample P2) resulted in a narrow MW distribution (I_p = 1.15), indicating the sufficient chain extension of OLA species onto the MePEG segments. It is interesting to note that $AlPO_4$-catalyzed formation of PEG–PLA (sample P4) also resulted in a major peak at high MW, and only a small amount of OLA species was detected on the SEC chromatograms, revealing the chain extension of OLA onto MePEG to form the PEG–PLA copolymer. Fig. 4 shows the FTIR spectra of the PEG–PLA copolymers. In the spectrum of PEG–PLA formed without catalysis (sample P1) or by $Al(OH)_3$ catalysis (sample P3), an O—H stretching band was observed at 3,500 cm^{-1}, probably due to the presence of unreacted LA oligomers [18]. In the literature, derivatives of Al and Sn (II) have been regarded as extremely versatile catalysts for the polymerization of lactide and other lactones [19–22]. A coordination-insertion mechanism was proposed in both cases, and the polymers are living systems. A coordination between OH-terminated PEG (nucleophiles) and the catalyst with vacant orbitals occurs, followed by an insertion of lactide into the polymer chain (Fig. 3A). Sn(II) catalysts were also applied in the melt–solid polycondensation of lactic acid [14,23,24], where the ring/chain equilibrium happens between OLA and lactide. In the present study, chain extension of OLA onto MePEG catalyzed by $AlPO_4$ is an efficient and convenient method of forming the PEG–PLA copolymer.

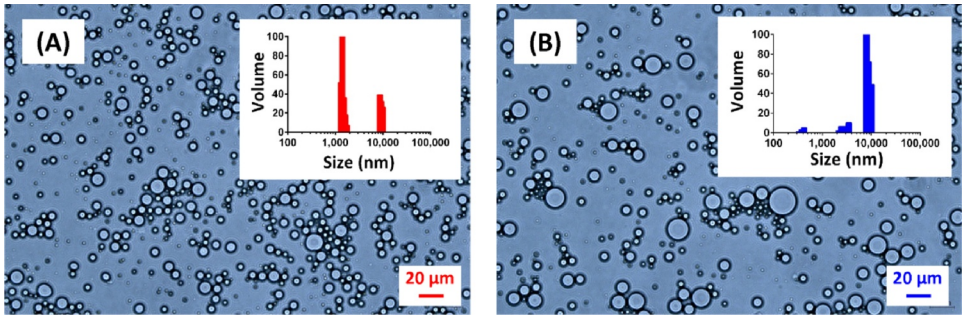

Fig. 6. Optical microscopy images and particle size distribution of the polymer-emulsified formulations made by **(A)** $SnOct_2$- and **(B)** $AlPO_4$-catalyzed PEG–PLA.

PEG–PLA copolymers were tested for their emulsifying ability. Without purification, the resulting products were then homogenized with squalene/aqueous mixtures. The amount of residual aluminum in final emulsified formulation is far below the recommended dosages in the registered aluminum-adjuvanted vaccines. As shown in Fig. 5, the PEG–PLA-stabilized squalene emulsion formed by $Al(OH)_3$ catalysis (sample P3) or without catalysis (sample P1) remained intact for only a few seconds and then separated into two phases, revealing that these compounds failed to stabilize the squalene/water interface; on the other hand, the PEG–PLA-stabilized emulsions formed by $SnOct_2$ catalysis (sample P2) and by $AlPO_4$ catalysis (sample P4) exhibited very stable and isotropic properties when they were stored for one month at ambient temperature. The quality of the emulsions was studied by redispersing them in a water bath and monitoring with an optical microscope and particle size analyzer. As shown in Fig. 6, the emulsion stabilized by P2 ($SnOct_2$-catalyzed PEG–PLA) has high affinity to water (oil-in-water emulsion); homogeneous fine particles of 1 μm in diameter were observed by optical microscopy and dynamic light scattering. Similarly, two different sizes with relatively small particles less than 1 μm and larger particles ~1–20 μm in diameter were observed in the emulsion stabilized by P4 ($AlPO_4$-catalyzed PEG–PLA). According to literature, the particles that were ~1 μm in diameter were recognized for uptake by antigen-presenting cells to facilitate the elicitation of appropriate immune responses [12]. We need to further assess the parameters tuning on emulsion characteristics for specific applications. With this potential in mind, further investigations are underway to extend platform technology for the design and fabrication of vaccine formulations for prophylactic and therapeutic uses. Such applications require an optimal emulsifying process in a consistent and reproducible manner which will be warranted to address these issues using a specific tumor-associated antigen therapy model and a prophylactic vaccine candidate against infectious disease.

4. Conclusions

Crystalline $Al(OH)_3$ and amorphous $AlPO_4$ were tested for their potential in protein adsorption and catalytic function. The morphology and antigen adsorption results revealed that aluminum hydroxide, rather than aluminum phosphate, is suitable to be a vaccine depot, which may play a crucial role in modulating the immune responses; on the other hand, it is of great interest that the chain extension of OLA onto MePEG catalyzed by $AlPO_4$ is an efficient and convenient method for the formation of the PEG–PLA copolymer. Concordantly, our results highlight the importance of morphology and antigen adsorption in the selection of aluminum-based adjuvants and offer insight into the design and synthesis of emulsion adjuvants.

CRediT authorship contribution statement

Yu-Jhen Cheng: Methodology, Data curation, Investigation, Visualization, Writing - original draft. **Chiung-Yi Huang:** Methodology, Data curation, Investigation. **Hui-Min Ho:** Resources, Methodology. **Ming-Hsi Huang:** Conceptualization, Investigation, Supervision, Writing - original draft, Writing - review & editing, Project administration, Funding acquisition.

Declaration of Competing Interest

The authors report no declarations of interest.

Acknowledgments

This work was supported by the National Health Research Institutes of Taiwan [grant number 109A1-IVPP19-014] and by the Ministry of Science and Technology of Taiwan [grant number MOST 106-2314-B-400-016-MY3]. The authors are grateful to Mr. Chih-Wei Lin for his help in preparing the materials and to Mr. Chun-Wei Chang, Institute of Biotechnology and Pharmaceutical Research of NHRI, for his help with polymer analysis.

References

[1] G. Del Giudice, K.J. Stittelaar, G. van Amerongen, J. Simon, A.D. Osterhaus, K. Stöhr, R. Rappuoli, Seasonal influenza vaccine provides priming for A/H1N1 immunization, Sci. Transl. Med. 1 (2009) 12re1, , https://doi.org/10.1126/scitranslmed.3000564.
[2] B. Gates, Responding to covid-19 - A once-in-a-century pandemic, N. Engl. J. Med. 382 (2020) 1677–1679, https://doi.org/10.1056/nejmp2003762.
[3] S. Shi, H. Zhu, X. Xia, Z. Liang, X. Ma, B. Sun, Vaccine adjuvants: understanding the structure and mechanism of adjuvanticity, Vaccine 37 (2019) 3167–3178, https://doi.org/10.1016/j.vaccine.2019.04.055.
[4] T.L. Flach, G. Ng, A. Hari, M.D. Desrosiers, P. Zhang, S.M. Ward, M.E. Seamone, A. Vilaysane, A.D. Mucsi, Y. Fong, E. Prenner, C.C. Ling, J. Tschopp, D.A. Muruve, M.W. Amrein, Y. Shi, Alum interaction with dendritic cell membrane lipids is essential for its adjuvanticity, Nat. Med. 17 (2011) 479–487, https://doi.org/10.1038/nm.2306.
[5] R.K. Gupta, Aluminum compounds as vaccine adjuvants, Adv. Drug Deliv. Rev. 32 (1998) 155–172, https://doi.org/10.1016/s0169-409x(98)00008-8.
[6] J.J. Lee, A. Shim, S.Y. Lee, B.E. Kwon, S.R. Kim, H.J. Ko, H.J. Cho, Ready-to-use colloidal adjuvant systems for intranasal immunization, J. Colloid Interface Sci. 467 (2016) 121–128, https://doi.org/10.1016/j.jcis.2016.01.006.
[7] F. Lu, H. HogenEsch, Kinetics of the inflammatory response following intramuscular injection of aluminum adjuvant, Vaccine 31 (2013) 3979–3986, https://doi.org/10.1016/j.vaccine.2013.05.107.
[8] P. Marrack, A.S. McKee, M.W. Munks, Towards an understanding of the adjuvant action of aluminium, Nat. Rev. Immunol. 9 (2009) 287–293 https://dx.doi.org/10.1038%2Fnri2510.
[9] B. Hansen, A. Sokolovsk, H. HogenEsch, S.L. Hem, Relationship between the strength of antigen adsorption to an aluminum-containing adjuvant and the immune response, Vaccine 25 (2007) 6618–6624, https://doi.org/10.1016/j.vaccine.2007.06.049.
[10] A. Colaprico, S. Senesi, F. Ferlicca, B. Brunelli, M. Ugozzoli, M. Pallaoro, D. O'Hagan, Adsorption onto aluminum hydroxide adjuvant protects antigens from degradation, Vaccine 38 (2020) 3600–3609, https://doi.org/10.1016/j.vaccine.2020.02.001.
[11] M.H. Huang, S.H. Dai, P. Chong, Mucosal delivery of a combination adjuvant comprising emulsified fine particles and LD-indolicidin enhances serological immunity to inactivated influenza virus, Microbes Infect. 18 (2016) 706–709, https://doi.org/10.1016/j.micinf.2016.06.007.
[12] W.L. Chen, S.J. Liu, C.H. Leng, H.W. Chen, P. Chong, M.H. Huang, Disintegration and cancer immunotherapy efficacy of a squalane-in-water delivery system emulsified by bioresorbable poly(ethylene glycol)-block-polylactide, Biomaterials 35 (2014) 1686–1695, https://doi.org/10.1016/j.biomaterials.2013.11.004.

[13] C.Y. Huang, C.H. Huang, S.J. Liu, H.W. Chen, C.H. Leng, P. Chong, M.H. Huang, Polysorbasome: a colloidal vesicle contoured by polymeric bioresorbable amphiphiles as an immunogenic depot for vaccine delivery, ACS Appl. Mater. Interfaces 10 (2018) 12553–12561, https://doi.org/10.1021/acsami.8b03044.

[14] C.Y. Huang, Y.J. Cheng, H.M. Ho, C.H. Huang, M.H. Huang, One-pot amphiphilic engineering of bioresorbable polymers for constructing colloidal vesicles and prolonging protein delivery, Polym. J. 52 (2020) 237–244, https://doi.org/10.1038/s41428-019-0267-3.

[15] S. Shirodkar, R.L. Hutchinson, D.L. Perry, J.L. White, S.L. Hem, Aluminum compounds used as adjuvants in vaccines, Pharm. Res. 7 (1990) 1282–1288, https://doi.org/10.1023/a:1015994006859.

[16] A. Boumaza, L. Favaro, J. Lédion, G. Sattonnay, J.B. Brubach, P. Berthet, A.M. Huntz, P. Roy, R. Tétot, Transition alumina phases induced by heat treatment of boehmite: an X -ray diffraction and infrared spectroscopy study, Solid State Chem. 182 (2009) 1171–1176, https://doi.org/10.1016/j.jssc.2009.02.006.

[17] S.L. Hem, H. Hogenesch, Relationship between physical and chemical properties of aluminum-containing adjuvants and immunopotentiation, Expert Rev. Vaccines 6 (2007) 685–698, https://doi.org/10.1586/14760584.6.5.685.

[18] S. Li, S. Anjard, I. Rashkov, M. Vert, Hydrolytic degradation of PLA/PEO/PLA triblock copolymers prepared in the presence of Zn metal or CaH_2, Polymer 39 (1998) 5421–5430, https://doi.org/10.1016/S0032-3861(97)10272-5.

[19] H.R. Kricheldorf, I. Kreiser-Saunders, A. Stricker, Polylactones 48. $SnOct_2$-initiated polymerizations of lactide: a mechanistic study, Macromolecules 33 (2000) 702–709, https://doi.org/10.1021/ma991181w.

[20] M. Bero, J. Kasperczyk, G. Adamus, Coordination polymerization of lactides, 3. Copolymerization of L,L-lactide and ε-caprolactone in the presence of initiators containing Zn and Al, Makromol. Chem. 194 (1993) 907–912, https://doi.org/10.1002/macp.1993.021940314.

[21] J. Kasperczyk, M. Bero, Coordination polymerization of lactides, 4. The role of transesterification in the copolymerization of L,L-lactide and ε-caprolactone, Makromol. Chem. 194 (1993) 913–925, https://doi.org/10.1002/macp.1993.021940315.

[22] H.R. Kricheldorf, J.M. Jonté, M. Berl, Polylactones 3. Copolymerization of glycolide with L,L-lactide and other lactones, Makromol. Chem. Suppl. 12 (1985) 25–38, https://doi.org/10.1002/macp.1985.020121985104.

[23] T. Maharana, B. Mohanty, Y.S. Negi, Melt–solid polycondensation of lactic acid and its biodegradability, Prog. Polym. Sci. 34 (2009) 99–124, https://doi.org/10.1016/j.progpolymsci.2008.10.001.

[24] S.I. Moon, Y. Kimura, Melt polycondensation of L-lactic acid to poly(L-lactic acid) with Sn(II) catalysts combined with various metal alkoxides, Polym. Int. 52 (2003) 299–303, https://doi.org/10.1002/pi.960.